

- R. A. Buhrman, and R. C. Richardson, *Phys. Rev. Lett.* **32**, 927 (1974).
- ³R. B. Kummer, R. M. Mueller, and E. D. Adams, *J. Low Temp. Phys.* **27**, 319 (1977).
- ⁴E. A. Schuberth, D. M. Bakalyar, and E. D. Adams, *Phys. Rev. Lett.* **42**, 101 (1979).
- ⁵H. Godfrin, G. Frossati, A. Greenberg, B. Hebral, and D. Thoulouze, *J. Phys. (Paris)*, Colloq. **41**, C7-125 (1980).
- ⁶T. C. Prewitt and J. M. Goodkind, *Phys. Rev. Lett.* **44**, 1699 (1980).
- ⁷T. Mamiya, A. Sawada, H. Fukuyama, Y. Hirao, K. Iwahashi, and Y. Masuda, *Phys. Rev. Lett.* **47**, 1304 (1981).
- ⁸R. A. Guyer, *Phys. Rev. A* **9**, 1452 (1974).
- ⁹W. P. Kirk, E. B. Osgood, and M. Garber, *Phys. Rev. Lett.* **23**, 833 (1969).
- ¹⁰J. R. Sites, D. D. Osheroff, R. C. Richardson, and D. M. Lee, *Phys. Rev. Lett.* **23**, 836 (1969).
- ¹¹T. C. Prewitt and J. M. Goodkind, *Phys. Rev. Lett.* **39**, 1283 (1977).
- ¹²D. M. Bakalyar, C. V. Britton, E. D. Adams, and Y. C. Hwang, *Phys. Lett.* **64A**, 208 (1977).
- ¹³Y. Morii, K. Ichikawa, T. Hata, C. Kanamori, H. Okamoto, T. Kodama, and T. Shigi, in *Physics of Ultralow Temperatures*, edited by T. Sugawara *et al.* (Physical Society of Japan, Tokyo, Japan, 1978), p. 196.
- ¹⁴T. Hata, S. Yamasaki, Y. Tanaka, and T. Shigi, *Physica (Utrecht)* **107B**, 201 (1981).
- ¹⁵M. Roger, J. M. Delrieu, and J. H. Hetherington, *J. Phys. (Paris)*, Colloq. **41**, C7-241 (1980).
- ¹⁶J. H. Hetherington, private communication.
- ¹⁷C. T. Van Degrift, *Physica (Utrecht)* **108B**, 1361 (1981).
- ¹⁸We determined our molar volumes from the melting pressure values of E. R. Grilly, *J. Low Temp. Phys.* **4**, 615 (1971).
- ¹⁹R. T. Johnson and J. C. Wheatley, *Phys. Rev. A* **1**, 1836 (1970).
- ²⁰T. P. Bernat and H. D. Cohen, *Phys. Rev. A* **7**, 1709 (1973).
- ²¹To be published.
- ²²R. A. Guyer, *J. Low Temp. Phys.* **30**, 1 (1978).
- ²³A. F. Andreev, *J. Phys. (Paris)*, Colloq. **39**, C6-1257 (1978).
- ²⁴G. Montambaux, M. Heritier, and P. Lederer, *J. Low Temp. Phys.* **47**, 39 (1982).
- ²⁵M. F. Panczyk and E. D. Adams, *Phys. Rev.* **187**, 321 (1969).
- ²⁶D. S. Greywall, *Phys. Rev. B* **15**, 2604 (1977).
- ²⁷L. Goldstein and J. C. Goldstein, *J. Low Temp. Phys.* **45**, 109 (1981).
- ²⁸Subsequent to the submission of this manuscript, W. P. Kirk offered preliminary results from new NMR susceptibility measurements that $\theta = 1.1 \pm 0.1$ mK at 24.02 ml/mole.

State-Dependent Recombination and Suppressed Nuclear Relaxation in Atomic Hydrogen

R. Sprik, J. T. M. Walraven, G. H. van Yperen, and Isaac F. Silvera

Natuurkundig Laboratorium der Universiteit van Amsterdam, 1018-XE Amsterdam, The Netherlands

(Received 24 February 1982)

A gas of 99.8% electron- and nuclear-spin-polarized hydrogen has been prepared. The surface and volume nuclear relaxation rates have been measured and the magnetic field dependence $(1 + 16.68/B)^2$ has been confirmed. The ratio of the surface recombination rate constants for collisions between atoms in hyperfine states, a - a and a - b , is measured to be 2.23(25). Nuclear relaxation on the surface has been suppressed by using ^3He to make an atomically flat surface.

PACS numbers: 67.40.-w, 67.70.+n

Since a gas of spin-polarized atomic hydrogen ($\text{H}\uparrow$) was first stabilized a few years ago¹ experimental efforts have been devoted to achieving sufficiently high densities or low temperatures to observe Bose-Einstein condensation (BEC). Densities, n , of just under $10^{17}/\text{cm}^3$ were soon obtained.^{2,3} These were limited by recombination of $\text{H}\uparrow$ to H_2 on the ^4He surfaces of the sample cell⁴⁻⁶: Because of the nonnegligible adsorption energy of $\text{H}\uparrow$ on He, $\text{H}\uparrow$ surface coverages (n_s) increase with decreasing temperature and the recombination (which increases with n_s ²) limits the

density.

Higher densities can be achieved by producing a state-selected gas of hydrogen. $\text{H}\uparrow$ has two hyperfine states $|a\rangle = |\uparrow\uparrow\rangle - \epsilon|\uparrow\downarrow\rangle$ and $|b\rangle = |\uparrow\downarrow\rangle$ (\uparrow , electron spin; \downarrow , nuclear spin), where $\epsilon \approx a/4\mu B$, with a the hyperfine constant, μ the Bohr magneton, and B the magnetic field. Statt and Berlinsky⁷ have pointed out that a nuclear-spin-polarized gas of pure b state ($\text{H}\uparrow\downarrow$) would have a much lower recombination rate as these atoms do not have admixtures of the electron "up" state. They suggested that this state might be achieved by prefer-

ential recombination of a -state atoms. The idea is that a - a collisions and a - b collisions can lead to recombination whereas b - b cannot. If the $a \rightarrow b$ nuclear relaxation time T_1 is much longer than the characteristic recombination time, the a state will be depleted leaving $H\downarrow$. Cline, Greytak, and Kleppner⁸ succeeded in producing a gas of $H\downarrow$ and measuring both the surface and the volume nuclear-spin-relaxation times T_1^s and T_1^v , respectively. The observed value $T_1^v \approx 13$ h was in agreement with theory.^{7,9} Van Yperen *et al.*¹⁰ attempted this experiment earlier but found very rapid relaxation, $T_1 \lesssim 10$ sec.

In this Letter we report on recent experiments in which we have created and studied $H\downarrow$ of purity up to 99.8%. A cell has been constructed with special care to eliminate surface magnetic impurities in the form of macroscopic grains (dimensions $\approx 0.1 \mu\text{m}$), believed to be the cause of the short T_1 's measured earlier. This cell, shown in Fig. 1, has a large area-volume ratio which enables the study of surface relaxation phenomena over a broad range of temperature. We describe how we have been able to strongly suppress surface relaxation with our special geometry which takes advantage of the predicted¹¹⁻¹³ anisotropy in the relaxation rate. This is vital for BEC as surface relaxation will be the limiting mechanism for achieving high densities. We also study the magnetic field dependence of T_1 . In addition, we have determined the important ratio of the recombination rate constants, K_{aa} for a - a collision and K_{ab} for a - b collisions,⁷ which, for simplicity, had earlier been assumed to be 1.

Both surface and volume nuclear-spin relaxation are of importance. The intrinsic surface relaxation rate $G_s \equiv (2T_1^s n_s)^{-1}$ is orders of magnitude faster than the volume rate G_v . Although both rates essentially arise from the magnetic dipolar interactions between atoms, the interaction can

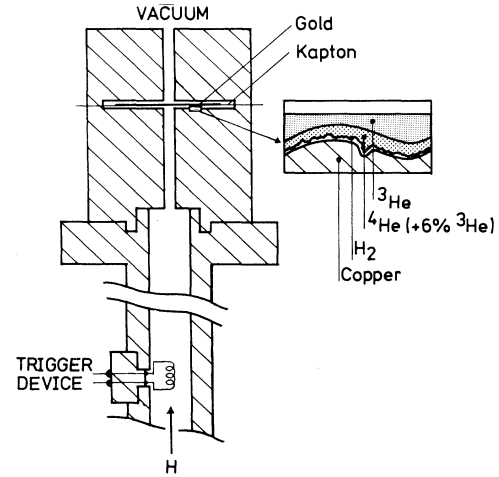


FIG. 1. Cross section of the hydrogen stabilization cell. The gold-plated Kapton is one plate of the capacitance pressure gauge. The inset shows what we believe to be a microscopic surface profile.

be averaged out by the motions. This motional averaging is less effective on the surface because the motions in two dimensions are slower than in three dimensions.¹¹ However, only very few atoms reside on the surface as can be seen from the adsorption isotherm for a mobile two-dimensional gas with a single bound state (such as $H\downarrow$ on He), $n_s = n\lambda \exp(\epsilon_a/kT)$, where $\lambda = (2\pi\hbar^2/mkT)^{1/2}$. The probability of finding an atom on the surface is $n_s A/nV = (A/V)\lambda \exp(\epsilon_a/kT)$, where A/V is the surface-to-volume ratio. Since atoms are rapidly exchanging between the surface and gas phases, to determine the effect of surface relaxation on gas-phase atoms we must multiply G_s by this factor which can be of the order 10^{-3} , rapidly increasing with decreasing temperature.

The rate equations for the decay of the density of a gas of $H\downarrow$ in states $|a\rangle$ and $|b\rangle$ are^{7,8} (valid for $kT \gg E_b - E_a$, the hyperfine splitting)

$$\frac{dn_a}{dt} = \frac{\varphi_a}{V} - \frac{n_a}{\tau_T} - G_s^{ie}(n_a - n_b) - (G_v + G_s^e)(n_a - n_b)(n_a + n_b) - 2K_{aa}^e n_a n_a - K_{ab}^e n_a n_b, \quad (1a)$$

$$\frac{dn_b}{dt} = \frac{\varphi_b}{V} - \frac{n_b}{\tau_T} + G_s^{ie}(n_a - n_b) + (G_v + G_s^e)(n_a - n_b)(n_a + n_b) - K_{ab}^e n_a n_b. \quad (1b)$$

Here $n_a + n_b = n$ is the total volume density; all coefficients superscripted with an e refer to surface phenomena and have been converted to effective volume terms. In Eq. (1a) the first term is the flux of a atoms filling volume V ; the second is the thermal leakage¹⁴ out of the cell which can be suppressed by making $B/T \gg 1$. The third term arises from magnetic impurities on the surface of the cell with $G_s^{ie} = G_s^i (A/V)\lambda \exp(\epsilon_a/kT)$, where G_s^i is the surface impurity nuclear-spin relaxation rate. Since ^3He atoms bear nuclear magnetic moments, relaxation due to a ^3He impurity or a pure ^3He surface would also be described by such a term. The fourth term describes relaxation due to binary collisions in the gas, G_v , or on the surface, $G_s^e = G_s (A/V)\lambda^2 \exp(2\epsilon_a/kT)$. As first described by Lagendijk,¹¹⁻¹³ the sur-

face relaxation rate is anisotropic with

$$G_s(B, T) = [G_{s,0}(\infty, T)\sin^2 2\theta + G_{s,2}(\infty, T)\sin^2 \theta(1 + \cos^2 \theta)](1 + 16.68/B)^2. \quad (2)$$

Here θ is the angle between the surface normal and the applied magnetic field; numerical evaluation shows that $G_{s,0} \gg G_{s,2}$. Note that for $\theta = 0$, $G_s = 0$. The fifth and sixth terms in Eqs. (1) describe surface recombination with $K_{aa}^e = K_{aa}(A/V)\lambda^2 \exp(2\epsilon_a/kT)$, where K_{aa} is the intrinsic surface rate; a similar definition exists for K_{ab} . In Eqs. (1) we ignore volume recombination.

For an accurate description of our experiments a detailed characterization of the geometry and surface conditions is necessary. The microscopic area A of the (rough) surface can be somewhat larger than the macroscopic or projected area A_p ; thus we define $A = \alpha A_p$. As a result of the magnetic field gradient and low temperature the gas has an inhomogeneous density distribution with an axial profile that depends exponentially on B/T .¹⁴ In our system, for small values of B/T the gas is spread over the cell, whereas for large values it is confined to the pancake-shaped region of the pressure gauge. For this reason we use effective volumes¹⁴ V^e and areas A^e in our analyses. $(A/V)^e$ varied between 40 and 140 cm^{-1} in our experiments. The gauge is designed to minimize the perpendicular area, A_\perp , corresponding to $\theta = 90^\circ$ in Eq. (2). The area here is $A_p = A_\parallel + A_\perp = (2.50 + 0.039) \text{cm}^2$. The upper surface is uncoated Kapton, and the lower is machined and etched copper. In the analyses in Fig. 2 we have used $A^e = A_p^e$. The rest of the system is similar to that shown in Fig. 1 of Ref. 9. A fine tungsten resistance wire is used to trigger¹ recombination of the H^\dagger .

We first measured decay curves (n vs t) for H^\dagger as a function of ^4He film thickness. For thin (undersaturated) films we observed a large first-order decay term. We assume that this arises principally from isolated O_2 or Fe impurities on or in the copper surface giving rise to a G_s^i term. A thick (\sim saturated) film of ^4He completely suppressed this.

The important ratio $\gamma = K_{aa}/K_{ab}$ can be determined if the relaxation can be ignored with respect to the recombination rates in Eqs. (1). Assuming $\varphi = 0$, $\tau_T = \infty$, and $n_{a0}/n_{b0} = 1$, one finds $n_\infty/n_0 = (2\gamma)^{(1-2\gamma)^{-1}}/2$, where the zero (∞) subscript refers to density at $t = 0$ (∞). The following interesting limits exist: $n_\infty/n_0 = 0.5$, 0.25, and 0 in the cases $K_{ab} = 0$, $K_{ab} = K_{aa}$, and $K_{aa} = 0$, respectively.

In Fig. 2(a) we show typical decay curves for H^\dagger with a thick ^4He coverage, demonstrating the

decay to an $\text{H}^\dagger\ddagger$ state. For curve 2 we rapidly fill the cell for several seconds so that $n_{a0} = n_{b0}$ and then allow the gas density to decay to its long-time value. We find $n_\infty/n_0 = 0.32$ after correcting for a small temperature rise of the cell during filling. This leads to a temperature-independent value of $\gamma = K_{aa}/K_{ab} = 2.23 \pm 0.25$ as measured for $T = 225, 250$, and 300 mK. In the limit of rapid relaxation, the recombination rate constant is the average of K_{aa} and K_{ab} . Using the results of Matthey, Walraven, and Silvera⁵ we find $K_{ab}B^2T^{-1/2} = 1.6(5) \times 10^{-7} \text{cm}^2 \text{T}^2/\text{K}^{1/2} \text{sec}$.

In Fig. 2(b) we plot our data for nuclear relaxation along with that of Cline, Greytak, and Kleppner (CGK).⁸ Each point represents a fit to a density decay curve, such as shown in Fig. 2(a), using Eq. (1). Our results are markedly different for ^3He and ^4He surfaces. The ^4He data are dominated by surface relaxation giving rise to an exponentially increasing relaxation with lowering of the temperature. Fitting the data by a straight line, we find $\epsilon_a/k = 0.89(6) \text{K}$ and $\alpha \langle G_s \rangle (1 + 16.68/B)^{-2} = 3.4(1.0) \times 10^{-13} \text{cm}^2/\text{sec}$. Here we use *one half* of the area of the pressure cell for reasons to be given later. We assumed the intrinsic surface relaxation rate (G_s) to be temperature independent. As shown by theory¹¹⁻¹³ G_s has a very weak temperature dependence, rather than being proportional to T as assumed by CGK.⁸ We note that because of their restricted temperature range and small A/V ratio, $G \equiv G_v + G_s^e$ is dominated by G_v , whereas our cell emphasizes G_s^e . To compare with the CGK-MIT results we evaluate their data using our value of ϵ_a (which increases their rate by 2.2) to find $1.8 \times 10^{-13} \text{cm}^2/\text{sec}$, or a factor 1.9 smaller than what we find.

The angular brackets on G_s refer to an average over the angle θ in Eq. (2). Defining $\bar{\theta}$ as the macroscopic value of θ , the CGK-MIT geometry has $\bar{\theta} = 90^\circ$ whereas our geometry has $\bar{\theta} = 0$. Ahn *et al.*¹³ have pointed out that the copper surface probably has a roughness of order 1–0.1 μm and it is more appropriate to consider the profile as a "muffin tin" surface. They average Eq. (2) using a section of a spherical surface subtending an angle φ . For $\varphi = 90^\circ$, $\alpha = 1.17$; G_s is totally dominated by $G_{s,0}$ with $\langle G_s \rangle / G_{s,0} \approx 0.39$ in the CGK-MIT geometry and 0.70 in ours. This provides a factor 1.8 and brings our results and the CGK-MIT results into good agreement. However, the

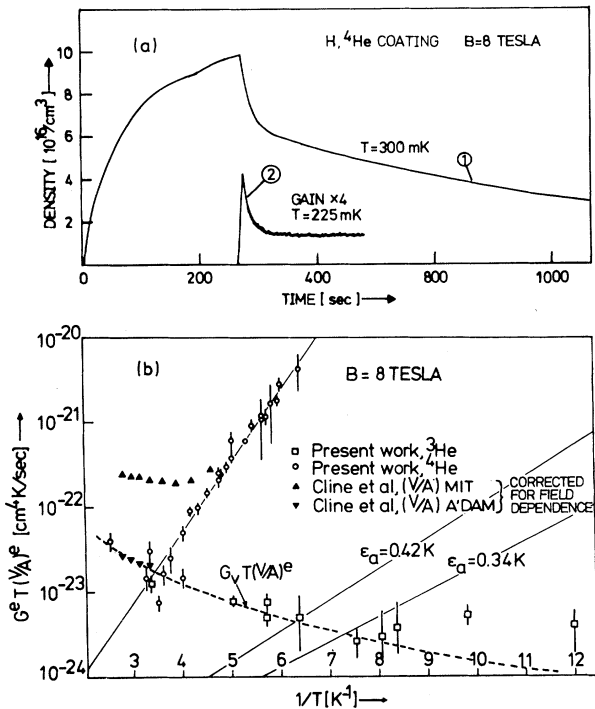


FIG. 2. (a) Decay of hydrogen to $H\uparrow\uparrow$. (b) The effective nuclear relaxation rate times $T(V/A)^e$ as a function of T^{-1} , for H on ${}^4\text{He}$ and ${}^3\text{He}$ - ${}^4\text{He}$ surfaces. The data of Cline, Greytak, and Kleppner are corrected to our conditions for comparison. The straight line is a fit to the data; its slope is $2\epsilon_a$. For the ${}^3\text{He}$ surface with a smaller ϵ_a , if surface relaxation were important, the data would rise linearly within the bound given by the two lines rising to the right. However, we only observe bulk relaxation. The dashed line is a fit to the ${}^3\text{He}$ data assuming $G_v \propto \sqrt{T}$.

theoretical value for $\langle G_s \rangle (1 + 16.68/B)^{-2}$ is $0.57 \times 10^{-14} \text{ cm}^2/\text{sec}$ for our geometry which is a factor 50 smaller than experiment (using $\alpha = 1.17$). A possible explanation is that because of the presence of the helium surface, H-H interactions will be modified so that relative motions are slowed, reducing the "motional narrowing" or increasing G_s .

We have also studied the dependence of G_s [Eq. (2)] on magnetic field and find reasonable agreement with theory.

Now we consider ${}^3\text{He}$ surfaces achieved from a mixture of ${}^3\text{He}$ - ${}^4\text{He}$. ${}^3\text{He}$ forms several monolayers on the ${}^4\text{He}$ as described by van Yperen *et al.*¹⁰ We might now expect a term G_s^i in Eq. (1) due to the ${}^3\text{He}$. However, this term is probably negligible as can be seen from scaling the dipolar interaction. For H- ${}^4\text{He}$, the H-H electron-nuclear dipole interaction is dominant and $(T_1^s)^{-1}$

$\propto (\gamma_e^H \gamma_n^H)^2 n_s^2$ whereas for H- ${}^3\text{He}$, the additional term due to ${}^3\text{He}$ is $(T_1^{3\text{He}})^{-1} \propto (\gamma_n^{3\text{He}} \gamma_n^H)^2 n_s n_{3\text{He}}$, where γ_n and γ_e are the nuclear and electronic gyromagnetic ratios. We find $(T_1^{3\text{He}})^{-1} / (T_1^s)^{-1} \approx 10^{-3}$, using $n_{3\text{He}} = 6.4 \times 10^{14} \text{ cm}^{-2}$ and $n_s = 10^{12} \text{ cm}^{-2}$. In Fig. 2(b) we also plot our data for G on ${}^3\text{He}$. Using the relaxation rate on ${}^4\text{He}$ and the measured values of ϵ_a on ${}^3\text{He}$ or ${}^3\text{He}$ - ${}^4\text{He}$ mixtures we would expect the data to fall within the bounds of the two lines for surface relaxation, contrary to observations. We identify the rate as volume relaxation with $G_v T^{-1/2} = 5.6(5) \times 10^{-21} \text{ cm}^3/\text{sec K}^{1/2}$ at $B = 8 \text{ T}$, in good agreement with the $5.3 \times 10^{-21} \text{ cm}^3/\text{sec K}^{1/2}$ of CGK on ${}^4\text{He}$, scaled to $B = 8 \text{ T}$. To understand why G_s is suppressed for ${}^3\text{He}$ and not for ${}^4\text{He}$, we note that in the latter case, the ${}^4\text{He}$ film in the pressure gauge will be of thickness $\sim 200 \text{ \AA}$ due to superflow properties of the film in the presence of gravity and the warmer lower sections of the cell.¹⁰ On the other hand, ${}^3\text{He}$ will be concentrated in the lowest-temperature part of the cell, the pressure gauge.

As a result of gravity the ${}^3\text{He}$ will level the surface of the lower (copper) side of the pressure gauge so that it is atomically flat (see Fig. 1, detail). The upper side, made of Kapton, will be covered with a thin ($\sim 200 \text{ \AA}$) ${}^3\text{He}$ - ${}^4\text{He}$ film. The Kapton surface examined by a scanning electron microscope appears flat with our highest spatial resolution of $\sim 100 \text{ \AA}$, with a low density of pits (diam $\lesssim 1 \mu\text{m}$) that may be filled by capillary condensation. Evidently the combination of Kapton and He film provides an atomically flat surface. In this case all of the A_\perp is atomically flat so that $\langle G_s \rangle \approx 0$. This implies that for pure ${}^4\text{He}$ surfaces we should just use the area of the copper, reducing the area of the pressure gauge by a factor 2, as used in the analyses. The maximum density achieved in this run with ${}^3\text{He}$ surfaces was $3 \times 10^{17}/\text{cm}^3$.

We thank O. H. Höpfner for technical aid and J. Kragten for chemical analyses of our copper. The financial support of the Stichting voor Fundamenteel Onderzoek der Materie is gratefully acknowledged.

¹I. F. Silvera and J. T. M. Walraven, Phys. Rev. Lett. **44**, 164 (1980).

²J. T. M. Walraven, I. F. Silvera, and A. P. M. Matthey, Phys. Rev. Lett. **45**, 449 (1980).

³R. W. Cline, D. A. Smith, T. J. Greytak, and D. Klep-

ner, Phys. Rev. Lett. 45, 2117 (1980).

⁴I. F. Silvera and J. T. M. Walraven, Phys. Rev. Lett. 45, 1268 (1980).

⁵A. P. M. Matthey, J. T. M. Walraven, and I. F. Silvera, Phys. Rev. Lett. 46, 668 (1981).

⁶M. Morrow, R. Jochemsen, A. J. Berlinsky, and W. N. Hardy, Phys. Rev. Lett. 46, 195 (1981), and 47, 455 (1981).

⁷B. W. Statt and A. J. Berlinsky, Phys. Rev. Lett. 45, 2105 (1980); J. M. Greben, A. W. Thomas, and A. J. Berlinsky, Can. J. Phys. 59, 945 (1981).

⁸R. W. Cline, T. J. Greytak, and D. Kleppner, Phys. Rev. Lett. 47, 1195 (1981).

⁹E. D. Siggia and A. E. Ruckenstein, Phys. Rev. B 23, 3580 (1981).

¹⁰G. H. van Yperen, A. P. M. Matthey, J. T. M. Walraven, and I. F. Silvera, Phys. Rev. Lett. 47, 800 (1981).

¹¹A. Legendijk, Phys. Rev. B 25, 2054 (1982).

¹²A. E. Ruckenstein and E. D. Siggia, Phys. Rev. B 25, 6031 (1982); B. Statt, Phys. Rev. B 25, 6035 (1982).

¹³R. M. C. Ahn, J. P. H. W. v.d. Eynde, C. J. Reuver, B. J. Verhaar, and I. F. Silvera, Phys. Rev. B 26, 452 (1982).

¹⁴J. T. M. Walraven and I. F. Silvera, Phys. Rev. Lett. 44, 168 (1980).